Electronic Supplementary Material (ESI) for Journal of Materials Chemistry A.

Supporting Information

A two-dimensionally microporous thiostannate with superior Cs^+ and Sr^{2+} ion-exchange property

Xing-Hui Qi, Ke-Zhao Du, Mei-Ling Feng, Jian-Rong Li, Cheng-Feng Du, Bo Zhang and Xiao-Ying Huang*

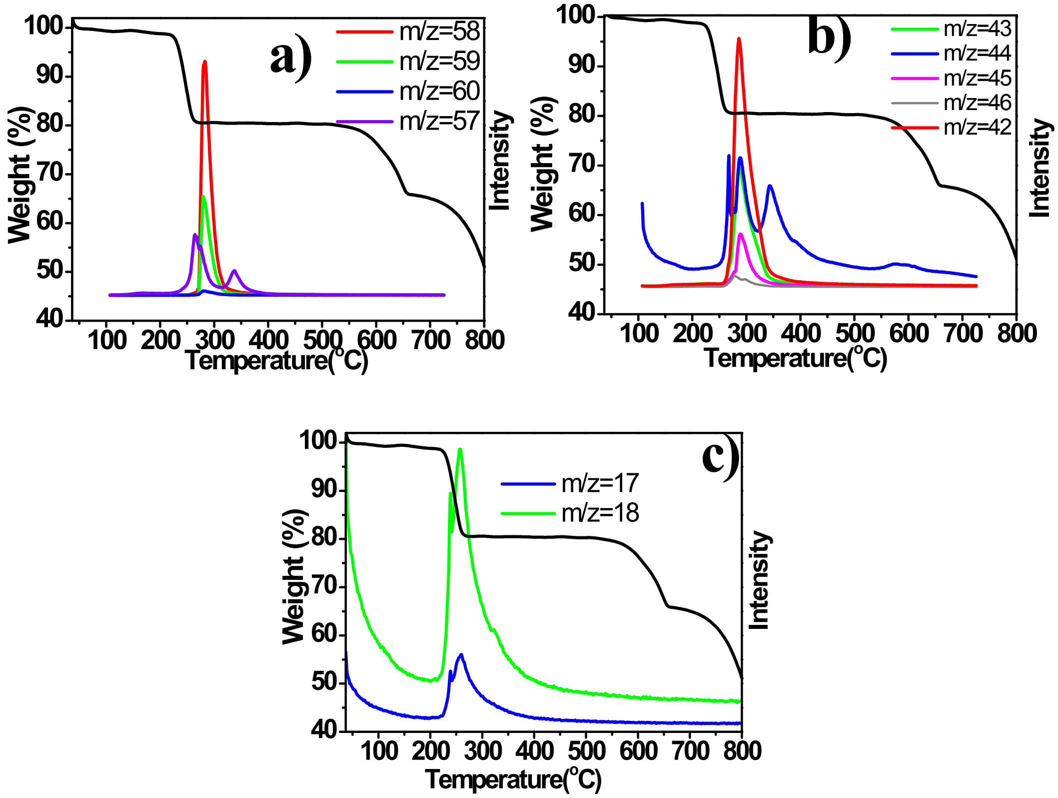

Fig. S1. The TG-MS spectra of FJSM-SnS crystals with the characteristic mass data of Me_3NH^+ (a), $Me_2NH_2^+$ (b) and H_2O (c).

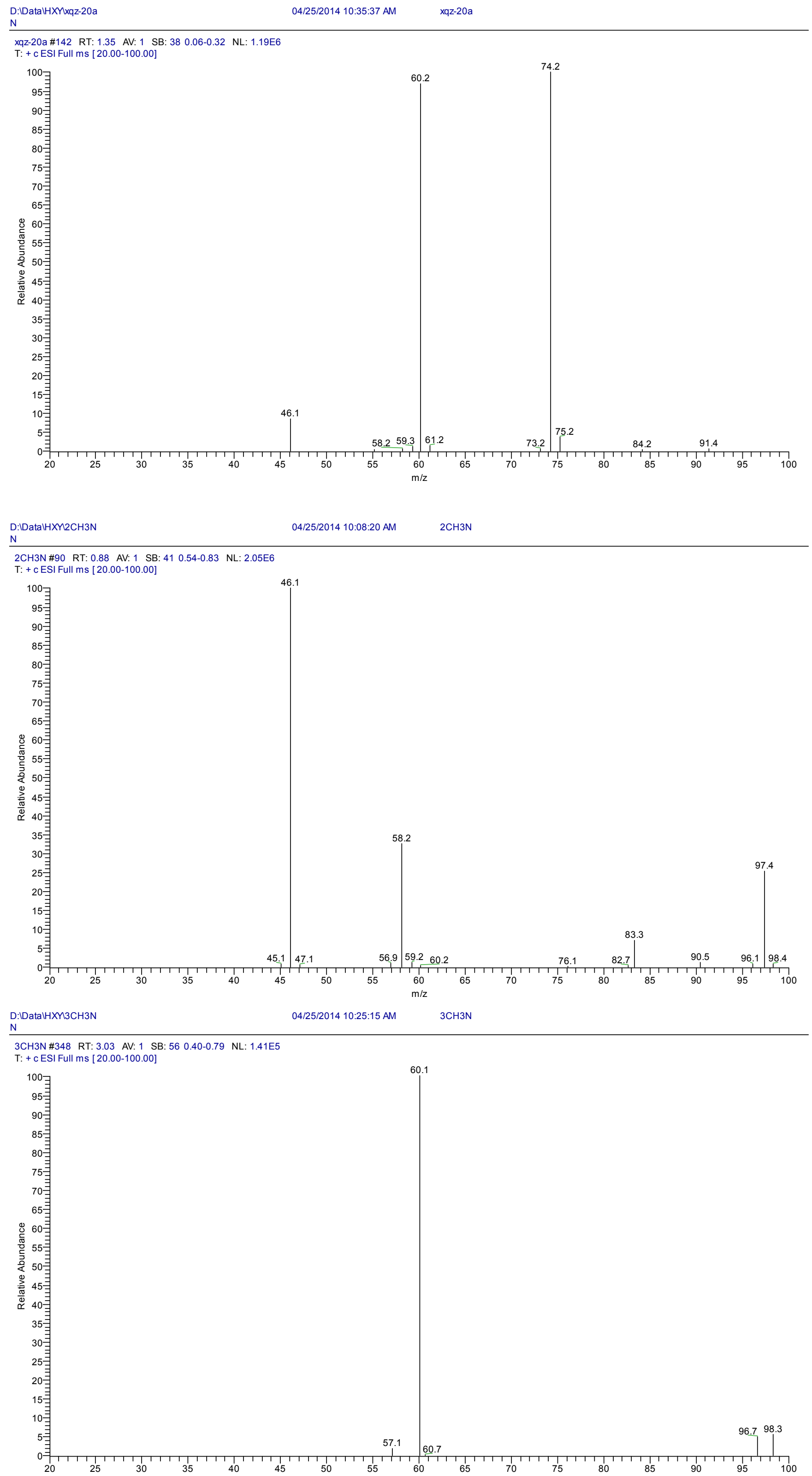

Fig. S2. Mass spectra of solution after solvetherml reaction (top), dimethylamine solution (middle) and trimethylamine solution (bottom).

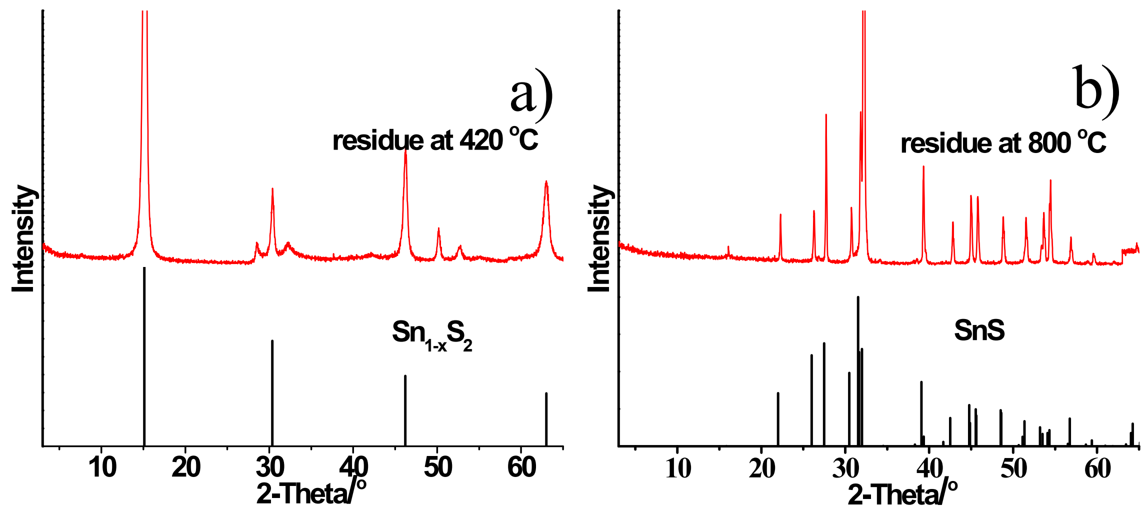

Fig. S3. The PXRD patterns of TG residues at 420 °C (a) and 800 °C (b) compared to the simulated $Sn_{1-x}S_2$ and SnS patterns, respectively.

The thermal stability of FJSM-SnS has been studied. Two cyclic heat treatments at 100 °C have been carried out, Figure S4a. The PXRD patterns are comparable to that of the pristine after heat treatments, Figure S4b, suggesting the structural stability of FJSM-SnS at the temperature range of ion-exchange experiments. In fact, the ability of Cs^+ removal is even improved a little after the heat treatment, Table S1.

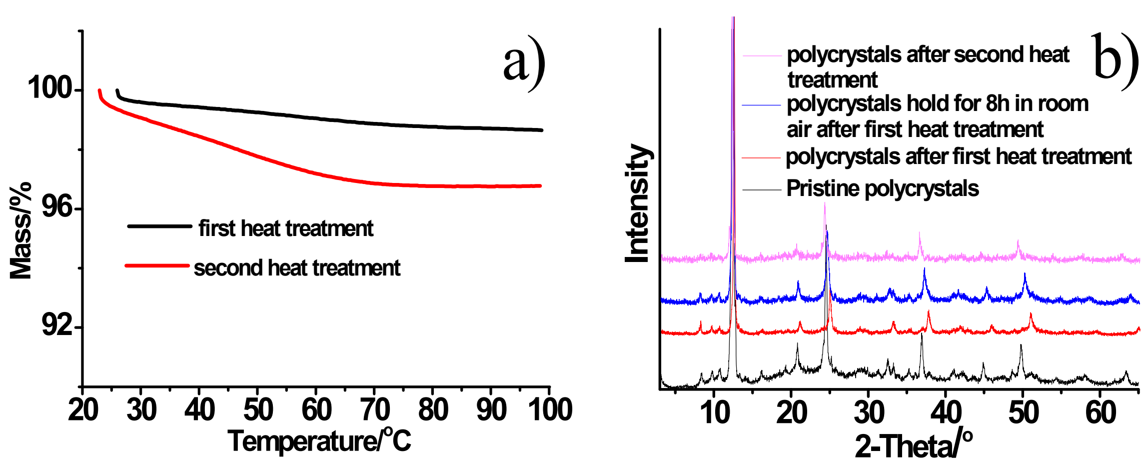

Fig. S4. a) The two cyclic heat treatments with 45 min homothermal time; b) the related PXRD patterns after heat treatment are in good agreement with that of the pritine FJSM-SnS crystals.

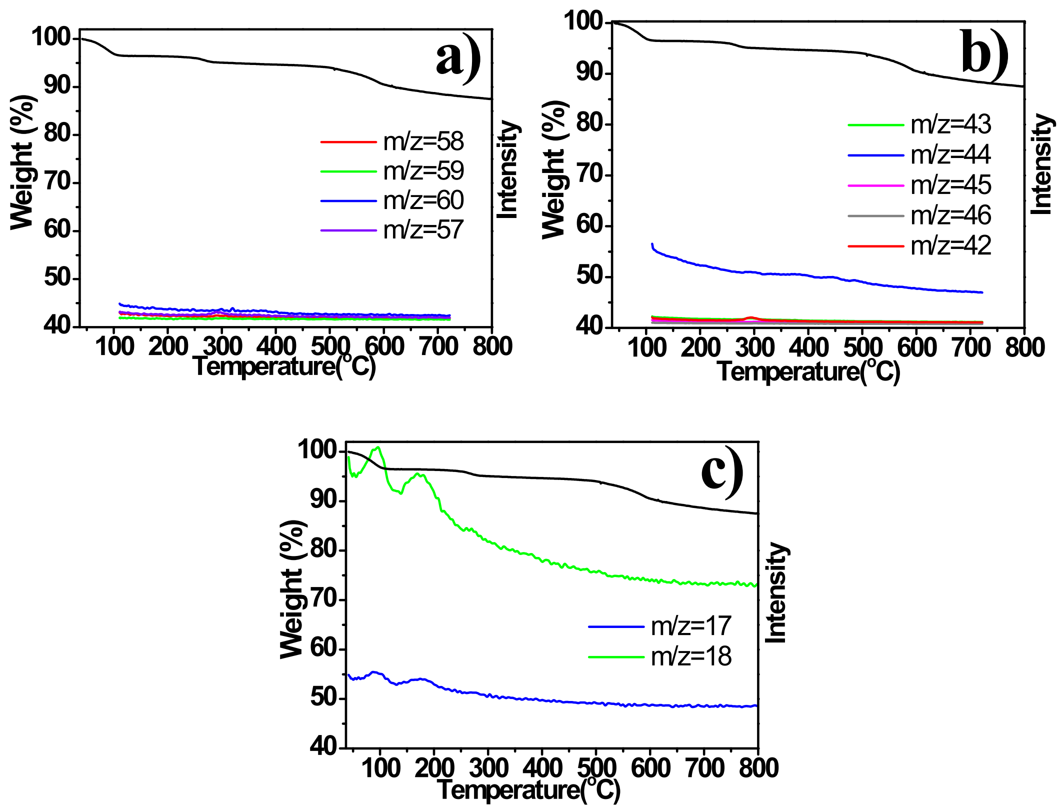

Fig. S5. The TG-MS spectra of the FJSM-SnS-Cs crystals with the characteristic mass data of Me_3NH^+ (a), $Me_2NH_2^+$ (b) and H_2O (c).

Element	Weight percentage	Atom percentage
C K	9.55	39.03
S K	22.23	34.03
Sn L	39.61	16.38
Cs L	28.61	10.57
Total	100.00	

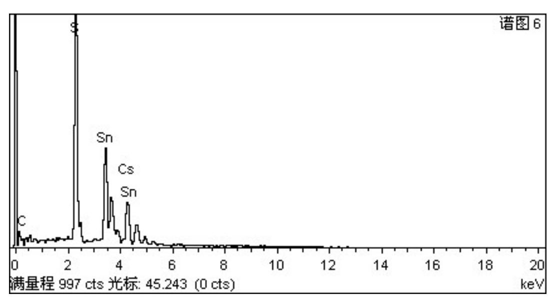

Element	Weight percentage	Atom percentage
C K	12.09	37.25
N K	5.87	15.50
S K	24.86	28.68
Sr L	6.73	2.84
Sn L	50.45	15.72
Total	100.00	

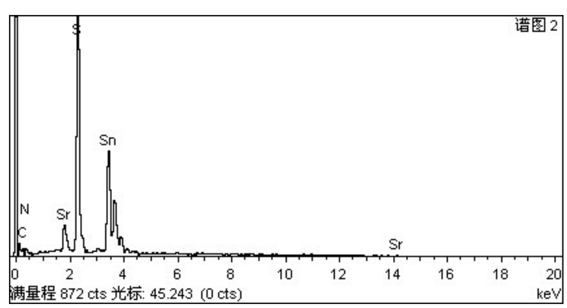

Fig. S6. The EDS diagrams and data for Cs^+ and Sr^{2+}-exchanged products, respectively. The results showed the ratio of Sn:Cs was close to 3:1.93 while that of Sn:Sr was 3:0.54, which further verified the large ion-exchange capacity for Cs^+ close to the theoretical one and smaller ion-exchange capacity for Sr^{2+}.

Table S1. The effect of heat treatment on the ion-exchange performance.

	m/ mg	*V* / mL	C_o / ppm	C_f / ppm	K_d / (mL/g)	Cs^+ Removal rate/%
FJSM-SnS	18.3	18	1.194	0.2805	3257	76.5
FJSM-SnS after heat treatment	18.3	18	0.9004	0.1873	3807	79.2

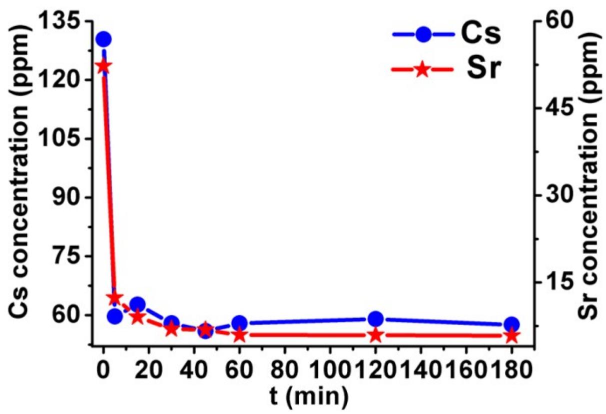

Fig. S7. Kinetics of Cs^+ and Sr^{2+} ion-exchange of FJSM-SnS at room temperature plotted as the Cs^+ and Sr^{2+} ion concentration (ppm) *vs* the time *t* (min), respectively. The solutions of Cs^+ (130.4 ppm) and Sr^{2+} (52.29 ppm) were prepared individually at neutral condition and V:m is 1000 mL/g (V = 10 mL, m = 10 mg). All the samples were carried out under 16-19 ^oC under magnetic stirring. Then we took one sample one time at different time of ion-exchange.

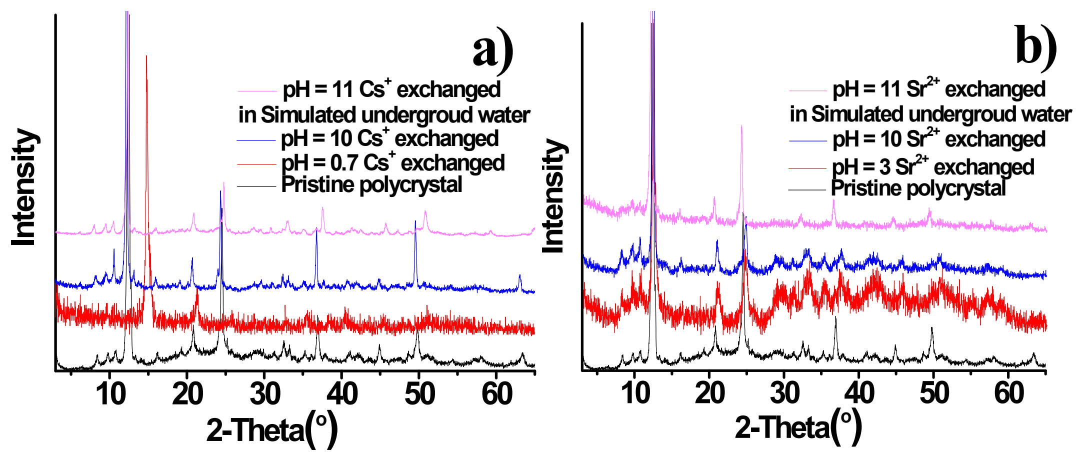

Fig. S8. PXRD patterns of the Cs^+ and Sr^{2+}-exchanged materials at extreme pH conditions.

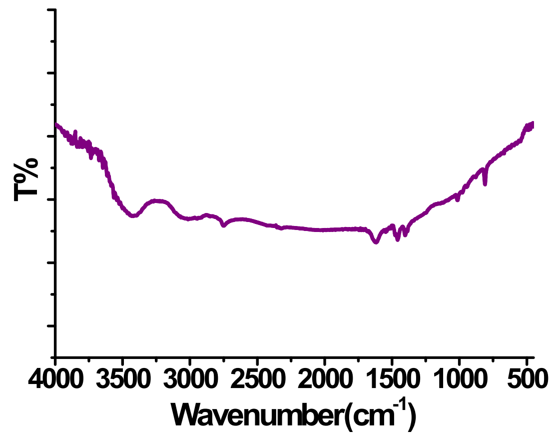

Fig. S9. IR spectrum of FJSM-SnS.

Fig. S10. Photograph of the crystals of as-synthesized FJSM-SnS in a typical large-scale synthesis.

Table S2. The ion-exchange experiments in simulated groundwater.

Metal cations	Conditions	C_o / ppm	C_f / ppm	K_d / (mL/g)
$Cs^+ + Ca^{2+} + Mg^{2+} + Na^+ + K^+$	pH~7, V:m ~ 100 mL/g	2.056 (Cs) 8.227 (Ca) 7.646 (Mg) 6.367 (K)	0.6535 (Cs) 0.4390 (Ca) 2.075 (Mg) 5.130 (K)	2.15×10^2 (Cs) 1.77×10^3 (Ca) 2.68×10^2 (Mg) 24 (K)
	pH~7, V:m ~ 1000 mL/g	2.159 (Cs)	1.652 (Cs)	3.07×10^2 (Cs)
	pH~11, V:m ~ 100 mL/g	1.984 (Cs) 7.878 (Ca) 8.315 (Mg) 5.574 (K)	0.8013 (Cs) 0.5483 (Ca) 1.853 (Mg) 5.481 (K)	1.48×10^2 (Cs) 1.34×10^3 (Ca) 3.49×10^2 (Mg) 1.7 (K)
$Sr^{2+} + Ca^{2+} + Mg^{2+} + Na^+ + K^+$	pH~7, V:m ~ 1000 mL/g	6.84 (Sr) 7.15 (Ca) 9.7 (Mg) 9.1 (K)	1.51 (Sr) 1.98 (Ca) 3.71 (Mg) 8.69 (K)	3.53×10^3 (Sr) 2.61×10^3 (Ca) 1.61×10^3 (Mg) 47 (K)
	pH~11, V:m ~ 1000 mL/g	6.22 (Sr) 5.32 (Ca) 7.53 (Mg)	3.81 (Sr) 4.55 (Ca) 5.82 (Mg)	6.32×10^2 (Sr) 1.70×10^2(Ca) 2.94×10^2 (Mg)

	76.51 (K)	43.66 (K)	7.52 ×10^2 (K)

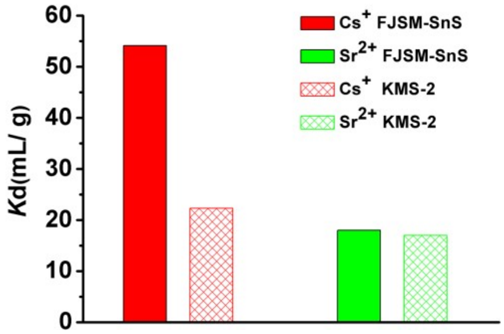

Fig. S11. The K_d of Cs^+ and Sr^{2+} in the simulated nuclear waste with the coexistence of 5 mol/L Na^+ ion and dilute Cs^+ or Sr^{2+} ions (KMS-2: Ref. 3, C_0 = 5.314 ppm for Cs^+, C_0 = 12.39 ppm for Sr^{2+}, V:m = 1000 mL/g, at 65 ^oC).

The ion-exchange performances in the simulated nuclear waste were explored. The solution with the coexistence of 5 mol/L Na^+ ion and dilute Cs^+ or Sr^{2+} ions was used to simulate nuclear waste. In the simulated nuclear waste, there are more than 10000-fold excess of Na^+ than Cs^+ and Sr^{2+}. The ion-exchange performances of FJSM-SnS could be greatly affected by the excessive Na^+ as KMS-1 and KMS-2.

Table S3. The competitive ion-exchange experiments of alkali metal cations.
(mole ratio, Cs^+: Rb^+: K^+: Na^+ = 1: 10: 10: 10)

Metal cations	C_o / ppm (initial concentration)	C_f / ppm (equilibrium concentration)	K_d / (mL/g) (distribution coefficient)
Na^+	80.26	71.08	1.3×10^2
K^+	129.3	117.83	0.97×10^2
Rb^+	257.7	230	1.20×10^2
Cs^+	47.32	30.93	5.30×10^2

Table S4. The competitive ion-exchange experiments of alkali-earth metal cations. (mole ratio, Sr^{2+}: Mg^{2+}: Ca^{2+}: Ba^{2+} = 1: 10: 10: 10)

Metal cations	C_o / ppm (initial concentration)	C_f / ppm (equilibrium concentration)	K_d / (mL/g) (distribution coefficient)
Mg^{2+}	7.25	1.96	2.67×10^3
Ca^{2+}	12.14	2.44	3.98×10^3
Sr^{2+}	3.4	0.48	6.08×10^3
Ba^{2+}	36.8	4.61	6.98×10^3

Table S5. The data in the ion-exchange chromatographic column experiment

Metal cations	*Volume/Bed volume*	C_o / ppm	C_t / ppm	C_t / pg·mL^{-1}
Cs^+	53.76344	12.03	0.4648	4.65×10^5
	89.60573	12.03	0.3941	3.94×10^5
	143.3692	12.03	0.4081	4.08×10^5
	179.2115	12.03	0.4053	4.05×10^5
	232.9749	12.03	0.4043	4.04×10^5
	268.8172	12.03	0.4109	4.11×10^5
	358.4229	14.52	0.2205	2.21×10^5
	465.9498	14.52	0.17	1.70×10^5
	555.5556	14.52	0.1996	2.00×10^5
	663.0824	14.52	0.2456	2.46×10^5
	720.4301	14.52	0.2709	2.71×10^5
	867.3835	14.52	0.3568	3.57×10^5
Sr^{2+}	53.76344	5.98	0.14	1.40×10^5
	89.60573	5.98	0.065	6.50×10^4
	143.3692	5.98	0.033	3.30×10^4
	179.2115	5.98	0.033	3.30×10^4
	232.9749	5.98	0.018	1.80×10^4
	268.8172	5.98	0.017	1.70×10^4
	358.4229	5.98	0.00853	8.53×10^3
	465.9498	5.98	0.00535	5.35×10^3
	555.5556	5.98	0.01067	1.07×10^4
	663.0824	5.98	0.00811	8.11×10^3
	720.4301	5.98	0.00581	5.81×10^3
	867.3835	5.98	0.00749	7.49×10^3